7. ANKARA INTERNATIONAL AEROSPACE CONFERENCE
11-13 September 2013 - METU, Ankara TURKEY

AIAC-2013-120

FREQUENCY DOMAIN SYSTEM IDENTIFICATION OF A UAV FROM FLIGHT TEST DATA

Orkun SIMSEK[1]
Middle East Technical University
Ankara, TURKEY

Ozan TEKINALP[2]
Middle East Technical University
Ankara, TURKEY

ABSTRACT

An overview of the ongoing research on airframe identification, based on frequency domain approach, of an UAV at Turkish Aerospace Industries, Inc. (TAI) is presented. The instrumentation and experiments design are also presented and discussed. The evaluation of handling qualities based on the identified system model is given and compared with the requirements.

Keywords: UAV, frequency domain system identification, handling qualities, transfer function modeling

INTRODUCTION

UAV, which is an acronym for Unmanned Aerial Vehicle, is generally used in both civil and military applications, where Unmanned Aerial Vehicle is defined by the Department of Defense (DoD) as 'powered, aerial vehicles that do not carry a human operator, use aerodynamic forces to provide vehicle lift, can fly autonomously or be piloted remotely, can be expendable or recoverable, and can carry a lethal or nonlethal payload' [U.S. DoD]. The main advantages of UAVs over manned aircrafts are that they are controlled remotely and/or autonomously and they are low cost and have low risk to operator life.

The terms, remote control and fully autonomous are difficult to get used to for pilots since controlling aircraft without sensing aircraft attitude is not easy. For this reason, UAVs are quite appropriate to use with automatic flight control systems, due to their low cost and limited risk of damage or harm. However, an accurate mathematical model of UAV dynamic is required for pilot training and control system design. Modeling using CFD or wind tunnel testing can be very labor intensive for a UAV project [Tischler, Remple, 2006]. The predicted results of these models may not match the actual aircraft accurately due to accumulated uncertainties and modeling simplifications. Therefore, the primary objective of this paper is to present a practical and accurate way of modeling identifying the flight dynamics of small fixed wing UAV.

System identification technique described in this paper is based on a frequency domain method, which is called as transfer function modeling. This modeling approach has been previously applied to NASA F-18 HARV (High Alpha Research Vehicle) [Morelli, 2000]. Unlike this study, Morelli has used multi inputs for identification and he has used different methods to obtain transfer functions. Another study on transfer function modeling has done by Morelli on a supersonic transport aircraft [Morelli, 2003]. In that study, Morelli has used frequency sweep to identify the aircraft dynamics. He obtained transfer function models of the aircraft are used to evaluate handling qualities.

Frequency domain system identification provides linear model of system dynamics. Since the aim of this study is to obtain an accurate linear model to be used in handling quality analysis and autopilot design. Frequency domain system identification has various advantages over time domain identification such as:

- Easy elimination of noise in the signal [Schoukens, Pintelon, Van Hamme, 1994]
- Identification of only frequency range of interest [Tischler, Remple, 2006]

---

[1] M.Sc. Student in a Aerospace Eng. Department, Email: e150354@metu.edu.tr
[2] Professor in Aerospace Eng. Department, Email: tekinalp@metu.edu.tr

- Independent measure of system excitation and data quality through coherence calculation [Tischler, Remple, 2006]
- Initial estimation of system state values is not required [Schoukens, Pintelon, Van Hamme, 1994]

In this study, a practical and systematical approach to identify aircraft model using flight test data is presented.

In the following, first the method used is summarized. It is followed by the description of the flight test experiments. The approach to transfer function-based identification is presented next, together with the presentation of the results obtained, and discussion. Finally conclusions are given.

BACKGROUND

Frequency domain system identification procedure is summarized by the flow chart given in Figure 1. The system identification procedure begins with the design of a flight test to excite the desired dynamic modes of the aircraft. Then, it continues with collecting data and data reconstruction. These parts of system identification are similar for both time domain and frequency domain identifications. For frequency domain, the system identification methods are based on spectral analysis that is consisting of:

- Fourier transform to generate frequency responses from time history data,
- Sampling to get exact representation of signal,
- Filtering to suppress the frequencies that are not of interest in the data
- Windowing to reduce the smearing of frequency content of the signal [Schoukens, Rolain, Pintelon, 2006].

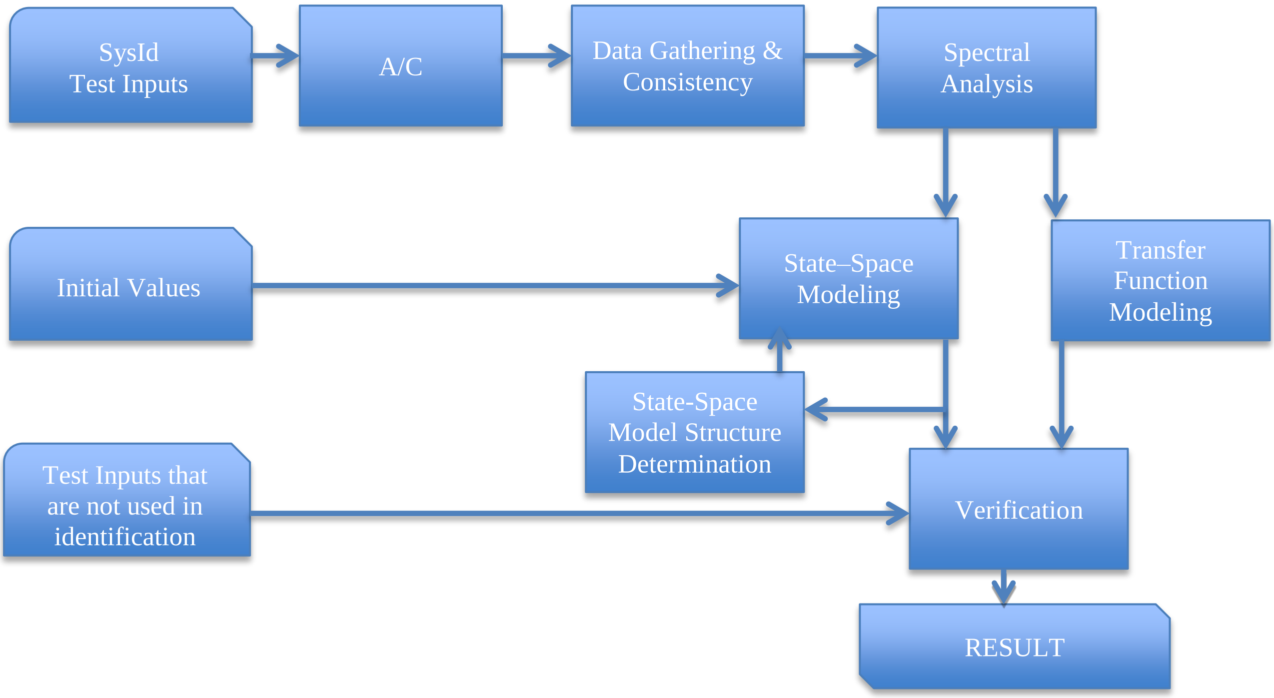

Figure 1: *Flow Chart of Frequency Domain System Identification*

After spectral analysis, there are two ways of identifying the system: transfer function modeling and state-space modeling. The verification is the last step of the procedure, and in this step, the identifying parameters are checked by the response of aircraft, which is excited by dissimilar set of test inputs with ones used in identification. In this manuscript, transfer function approach is used.

The frequency response function H (f) is the ratio of the output to the input Fourier transforms. The frequency response function equation is written as [Tischler, Remple, 2006]:

$$H(f) = \frac{Y(f)}{X(f)} \quad (1)$$

Fourier transform of a signal for a discrete and defined time interval (data records) is written as [Tischler, Remple, 2006]:

$$X(f_k) = X(k\Delta f) = \Delta t \sum_{n=0}^{N-1} x_n e^{-j2\pi(kn)/N} \quad (2)$$

where,

$X(f_k)$: Fourier coefficients, for k=0,1,2,…,N-1 x_n : time-domain data record, for n=0,1,2,…,N-1

Δt : time increment Δf : frequency resolution

N : number of discrete frequency points

The system identification algorithm main aim is minimizing the cost function given as [Tischler, Remple, 2006]:

$$J = \frac{20}{n_w} \sum_{w_l}^{w_{n_w}} W_\gamma \left[W_g\left(|\hat{T}_c| - |T|\right)^2 + W_p\left(\angle\hat{T}_c - \angle T\right)^2 \right] \quad (3)$$

where

W_γ, W_g, W_p : identification weighting for coherence function, magnitude and phase, respectively

$\angle$, | | : phase (deg) and magnitude (dB) T: frequency response matrix of identification model

w : frequency (rad/s) n: number of states in linear time-invariant system

EXPERIMENT DESIGN

Platform

Pelikan, used in this study, is a TAI developed and instrumented test platform. It has high-wing configuration, 2piston-prop engines (1 pusher, 1 tractor), tricycle landing gear system and boom mounted tail arrangement. The specifications and a sketch of Pelikan are given in Figure 2.

Parameter	Value
Length	3,3 m
Wing Span	4,0 m
Wing Chord	0,39 m
Wing Area	1,5 m^2
MTOW	65 kg
Ixx	16 kgm^2
Iyy	40 kgm^2
Izz	55 kgm^2

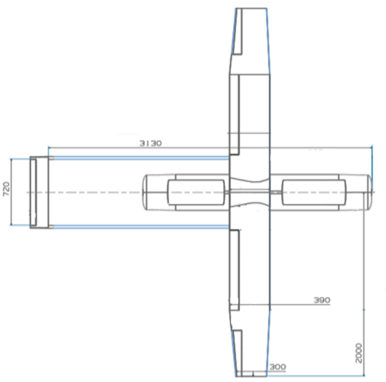

Figure 2: *Specifications of Pelikan UAV*

Instrumentation

Jategaonkar indicates that ''If it is not in the data, it cannot be modeled'' [Jategaonkar, 2006]. This basic rule makes input design for tests and instrumentation important. The importance of instrumentation arises from that the quality of sensor specifies the data characteristics like accuracy, noise, etc. In addition, some features of data recording, such as sample rate and filtering are important since they directly affect the available information in the data. According to the Shannon's sampling theorem, sample rate should be at least twice of the maximum frequency present in the signal. However, in reality more than that is necessary. The filters utilized may cause unreal phase resulting into parameter estimations with bias [Tischler, Remple, 2006]. Therefore, in Pelikan, digital filters with same cut-off frequency of 50 Hz is applied to all sensor measurements, such as, GPS/INS(EGI), air data boom (pitot) measurements, servo commands, and servo encoders. The measured variables are given in Table 1.

Table 1: *List of Measured Quantities*

	Measured Quantity		Measured Quantity		Measured Quantity		Measured Quantity
EGI Data	ax	**Pilot Commands**	Aileron Command	**Air Data**	V	**Servo Encoder**	Left Aileron Position
	ay		Elevator Command		α		Right Aileron Position
	az		Ruddervator Command		β		Left Elevator Position
	p		Throttle Command		h		Right Elevator Position
	q						Left Ruddervator Position
	r						Right Ruddervator Position
	ϕ						Rpm
	θ						
	ψ						

The GPS/INS system used in A/C includes a MEMS based Inertial Measurement Unit (INS), a GPS receiver and a pressure sensor. In addition, this system has a built in Extended Kalman Filter. In Figure 3, the block diagram of EGI is given:

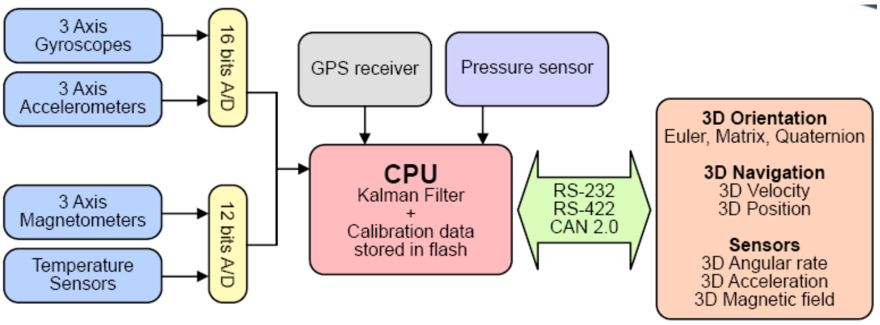

Figure 3: *The Block Diagram of EGI*

Air data test boom has total and static pressure ports, angle of attack and angle of sideslip vanes. Its shape and the location on the A/C are presented in Figure 4.

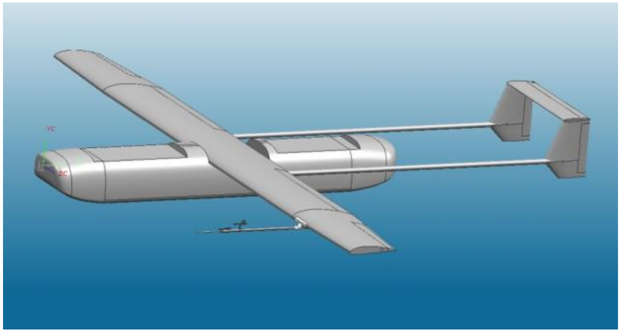

Figure 4**:** *CAD Model of the Pelikan*

Flight Test Input Design

The inputs used in frequency domain are separated in two main parts:

- Inputs used for identification
- Inputs used for verification

Inputs used for identification are generally frequency sweeps for frequency domain system identification. If it is not applicable, several multi-inputs like 3-2-1-1 input or doublets may be applied in series [Morelli, 2003].

Inputs used for verification are generally doublets, multi inputs like 3-2-1-1 and 1-2-1. The important thing for verification inputs is that they must be dissimilar than inputs used in identification to ensure that the identified model is accurate and robust [Williams, Ham, Tischler, 1995].

Frequency sweep refers to a class of control inputs that has a quasi-sinusoidal shape of increasing frequency. Tischler remarks four important points while planning frequency sweep tests [Tischler, Remple, 2006]:

1. Before and after frequency sweeps, there are nearly 3s trim durations to get trim states of control inputs and responses

2. The frequency sweep starts with two long period control inputs to get data about low frequency dynamics like phugoid.
3. In frequency sweep, the increase in frequency is performed smoothly to prevent rushing through mid-frequencies.
4. While applying frequency sweeps, the aircraft oscillations are roughly symmetric and responses are near trim values. Aircraft responses in the range of ±5-15 deg in angular attitudes and ±5-15 deg/s in angular rates and ±5-10kts in velocity and the inputs in the range of ±10-20% of control input are intended to obtain in frequency sweeps.

In flight tests of Pelikan, there are practical constraints while applying frequency sweeps. For a racetrack pattern, the flight leg where identification tests are performed is 25 seconds long. Therefore, a sweep is performed in 25 seconds. The trim duration takes 5 seconds therefore the frequency sweeps lasts nearly 20 seconds.

While applying frequency sweep input, exact sinusoidal input shape is not required also is not desirable since irregularities ensure a broader bandwidth of excitation, and non-repeatability of the input waveform improves the overall info content when concatenated sweep records are formed [Tischler, Remple, 2006]. However, for long period inputs, input shape is quite important since the aircraft responses can be diverged from trim condition.

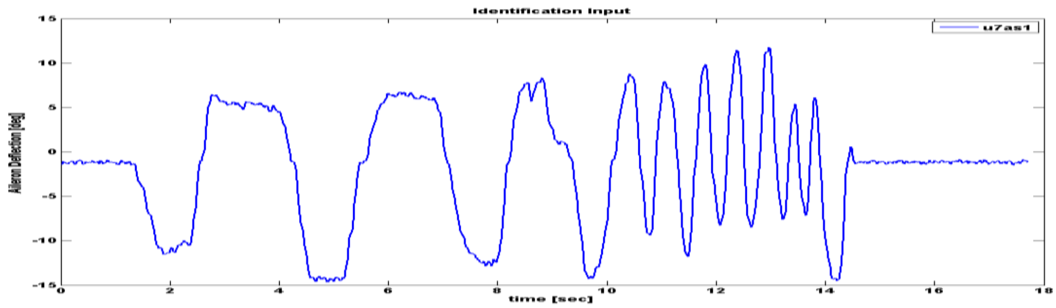

Figure 5: *Aileron Identification Inputs*

The aims of the verification are [Tischler, Remple, 2006]

- to check the accuracy of the identified model by comparing the time domain response predictions and measured flight data.
- to check the robustness of the identified model by comparing the time domain response predictions and measured flight data.

The input used in identification is used for accuracy verification; however, for robustness analysis, dissimilar inputs are used. In this study, doublets and 1-2-1 multi inputs are used as dissimilar inputs

Doublets are applied moving control abruptly in one direction, then the input is kept fix for certain time Δt, after that control moved abruptly to other direction, after another Δt time, it moves back to the neutral position of control input [Jategaonkar, 2006]. The frequency content of the doublet depends on Δt. The smaller it is, the larger its spectrum spreads. Some of the doublets applied in Pelikan flight test given in Figure 6, which is obtained using the encoder data of rudder deflections.

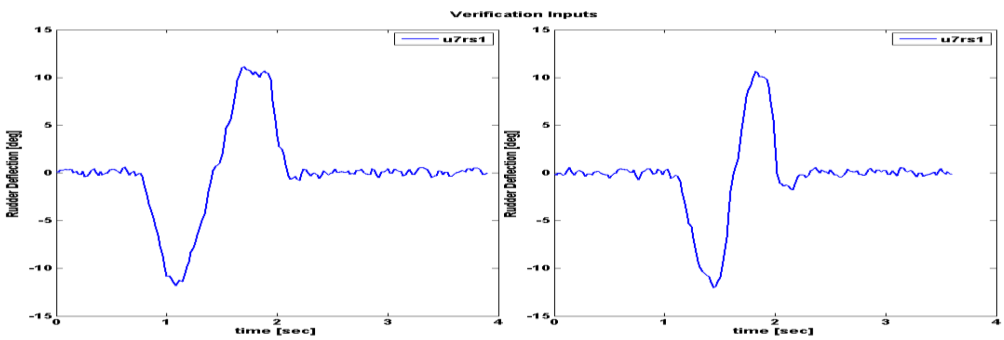

Figure 6: *Rudder Doublets*

Extending the logic that progressing from single-step input to two-step input (doublet) leads to a spread of the power spectrum; therefore, much broader band signal is achieved through a multistep input. 3-2-1-1 is one of the multistep inputs and it is 7Δt long and includes positive and negative equal amplitude steps. 1-2-1 input is generally used for lateral system identification, especially for aileron inputs [Jategaonkar, 2006]. In Figure 7, first subplot shows aileron 1-2-1 input applied in flight test and second subplot shows aileron doublet.

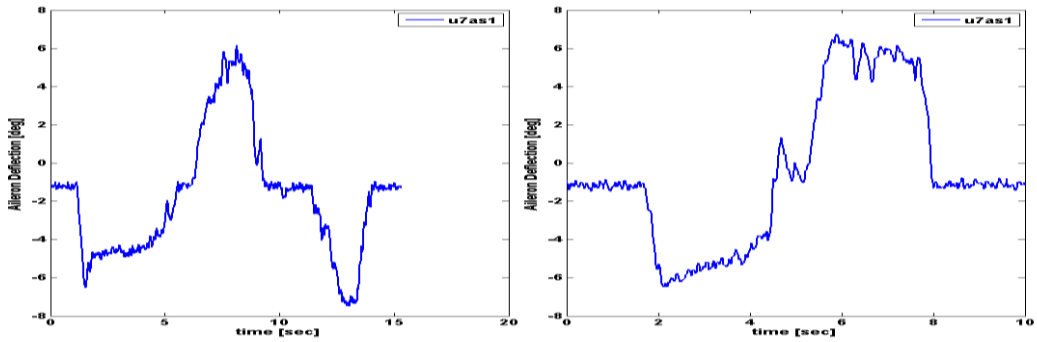

Figure 7: *Aileron 1-2-1 and Doublet Input Examples*

Flight Path Reconstruction

Before using the flight test data, it is often necessary and timesaving to verify whether the recorded data are compatible or not. The corruption in the data caused by systematic errors like scale factors, zero shift biases and time lags is determined before identification process. Verifying the compatibility of measured data is based on the use of kinematic relationships. A detailed explanation is found in [Klein and Morelli, 2006] and a good example is found in [Klein, 1977] about compatibility check. In compatibility check, the main aim is matching measured parameter with its computed value using its kinematic equation where the parameters take their measured values. For example in (4), measured y is matched by result of y function where parameters in y function take their measured values. This matching process is also termed as Flight Path Reconstruction (FPR). In general, there are two approaches to flight path reconstruction [Jategaonkar, 2006]. A rigorous one in the stochastic framework based on the extended Kalman filter, while a simpler one in the framework of deterministic systems based on the output error method.

When a simple sensor model is considered, the sensor model equation is given in terms of scale factor, bias and time delay as,

$$\mathrm{y_m(t) = K_y y(t-\tau) + \Delta y} \tag{4}$$

where, K_y is the scale factor, Δy is the unknown instrument bias and y_m and y are the measured output and computed output, respectively.

Kinematic equations are valid for parameters values at CG position. Therefore, before reconstruction is applied, the measured parameters must be corrected to CG position since sensors are not put at CG. For accelerometer measurement correction, the linear accelerations at the center of gravity (a_x^{CG}, a_y^{CG}, a_z^{CG}) are computed from the accelerations measured by the sensor (a_{xm}^s, a_{ym}^s, a_{zm}^s) at a point away from the CG (x_{sCG}, y_{sCG}, z_{sCG}) through the following relation:

$$a_x^{CG} = a_{xm}^s + (q^2+r^2)x_{sCG} - (pq-\dot{r})y_{sCG} - (pr-\dot{q})z_{sCG} - \Delta a_x \tag{5}$$

$$a_y^{CG} = a_{ym}^s - (pq+\dot{r})x_{sCG} + (p^2+r^2)y_{sCG} - (qr-\dot{p})z_{sCG} - \Delta a_y \tag{6}$$

$$a_z^{CG} = a_{zm}^s - (pr-\dot{q})x_{sCG} - (qr+\dot{p})y_{sCG} - (p^2+q^2)z_{sCG} - \Delta a_z \tag{7}$$

The biases in the measurements of (a_{xm}^s, a_{ym}^s, a_{zm}^s) are denoted by (Δa_x, Δa_y, Δa_z) and the angular rates (p, q, r) are given by ($p_m - \Delta p$, $q_m - \Delta q$, $r_m - \Delta r$) obtained from the measured rates (p_m, q_m, r_m) corrected for the biases (Δp, Δq, Δr). The variables ($\dot{p}, \dot{q}, \dot{r}$) are obtained by numerical differentiation of the measured angular rates. Similarly, the speeds are measured using nose boom; therefore, before using these in reconstruction, they are corrected for CG position using (8), (9) and (10).

$$u_{NB} = u - (r_m - \Delta r)y_{NBCG} + (q_m - \Delta q)z_{NBCG} \tag{8}$$

$$v_{NB} = v - (p_m - \Delta p)z_{NBCG} + (r_m - \Delta r)x_{NBCG} \tag{9}$$

$$w_{NB} = w - (q_m - \Delta q)x_{NBCG} + (p_m - \Delta p)y_{NBCG} \tag{10}$$

When the flight test data are analyzed, it is noticed that the measured variables are too noisy to use in an analysis. Therefore, Savitzky-Golay Filter is used to eliminate the noise in the data. This method of data smoothing based on local least-squares polynomial approximation. They demonstrated that least square smoothing reduces noise while maintaining the shape and height of waveform peaks [Schafer, 2011]. The filter may be applied to speed, angular speed, control surface deflections angel of attack and angle of sideslip measurements.

In this study, output error method (OEM) is used for flight path reconstruction and the model for this method is summarized in Table 2. The estimated values of unknown variables are achieved by matching measured and calculated variables [Jategaonkar, 2006].

Table 2: *Variables Used in OEM*

State Variables	$u, v, w, \phi, \theta, \psi, h$
Measurement Variables	$V_m, \alpha_m, \beta_m, \phi_m, \theta_m, \psi_m, h_m$
Input Variables	a_x, a_y, a_z, p, q, r
Estimation (Unknown) Variables	$\Delta a_x, \Delta a_y, \Delta a_z, \Delta p, \Delta q, \Delta r, K_\alpha, \Delta\alpha, K_\beta, \Delta\beta$

Flight path reconstruction (FPR) is applied for longitudinal and lateral/directional motion separately. In longitudinal motion FPR, the scale factor and bias of AoA are estimated, and in lateral/directional motion, the scale factor and bias of AoS are estimated using Eqn (4). Reconstructed values of AoA and AoS values are shown in Figure 8 by comparing with measured values. In the rest of the study, the reconstructed values of AoA and AoS are used in identification. The obtained scale factor values for AoA and AoS are 1.32 and 1.107 respectively and the biases for AoA and AoS are calculated as -0.0017 rad and -0.014 rad respectively.

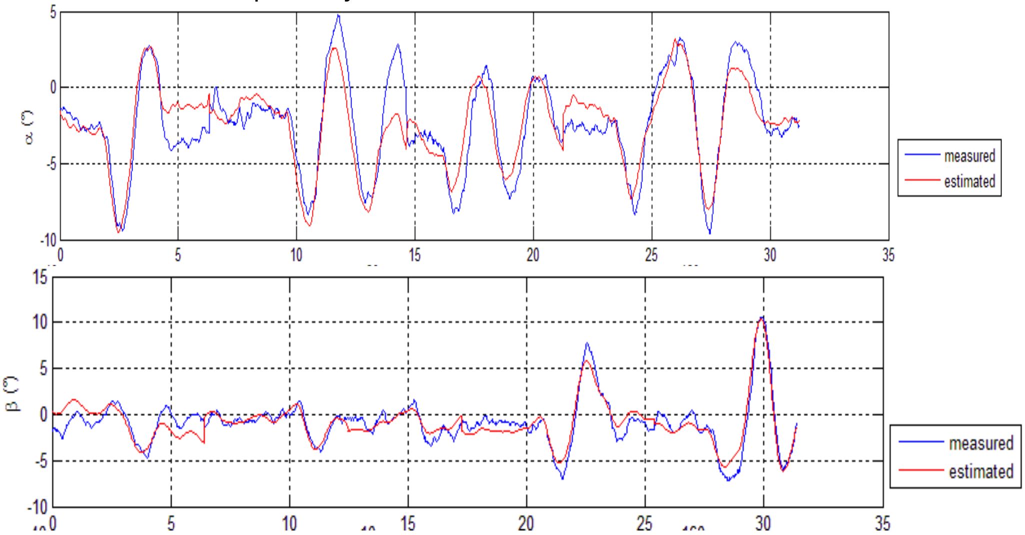

Figure 8: *Measured and Estimated AoA and AoS Value Comparison*

RESULTS AND DISCUSSION

Transfer function model of a system represents input-output relation in that system. Such a transfer function may be written as,

$$T(s) = \frac{(b_0 s^m + b_0 s^m + \cdots + b_m)\, e^{-\tau_{eq} s}}{(s^n + a_1 s^{n-1} + \cdots + a_n)} \qquad (11)$$

In this model, the identified parameters are coefficients of numerator and denominator and an equivalent time delay, instead of stability and control derivatives of the system. While, the numerator and denominator give the relation between input and output, the time delay represents the effect of the high-frequency dynamics and actual delay in that system.

Model Structure Selection

The model structure determination is important for transfer function modeling, since model structure determines response characteristics to inputs. Therefore, correct model structure is a baseline for the identification. If it is identified correctly, then the rest is estimating the transfer function coefficients. Since transfer functions do not provide any information about physical structure of the system, the model structure is determined using following steps by concerning the possible physical structure of the system:

- the input-output pairs,
- frequency range of interest,
- order of numerator and denominator,
- equivalent time delay

Then the identifiable parameters, which are coefficients of numerator and denominator and time delay τ_{eq}, are estimated.

Input-Output Pairs

For a dynamic mode, which will be identified, proper input-output pair(s) for that mode must be selected. The dominant pairs that have most available information about the dynamic mode are found by:

- using dominant pairs in approximations like short period approximation etc.
- using pairs which have high coherence.

According to these explanations, in this study, β/δr is chosen for directional motion, p/δa is chosen for lateral motion, α/de is chosen for short period motion.

Interested Frequency Range

The frequency range used in identification is defined by frequency range of interest where frequencies contain enough information for identification (frequencies where coherence is higher than 0.6) .For the handling quality analysis, the frequency range of interest is taken as 0.1 – 10 rad/s [Tischler, Remple, 2006]. If the aircraft is excited properly through the desired frequency range and the input/output pairs have high coherence for the whole frequency range of interest. If this transfer function model is used for flight control design, the model must be accurate for frequencies near crossover frequency ω_c, generally 0.3 ω_c to 3 ω_c [Tischler, Remple, 2006].

Order of Numerator and Denominator

The order of numerator and denominator is the main factor that represents response characteristics. An appropriate transfer function model of fixed wing dynamics is based on the classical flight mechanics response. Therefore, for the pairs p/δ_a, β/δ_r and α/δ_e, the following transfer function models are chosen as [Roskam, 2001]:

$$\frac{p}{\delta_a}(s) = \frac{s(A_\emptyset s^2 + B_\emptyset s + C_\emptyset)}{A_2 s^4 + B_2 s^3 + C_2 s^2 + D_2 s + E_2} \tag{12}$$

$$\frac{\beta}{\delta_r}(s) = \frac{A_\beta s^3 + B_\beta s^2 + C_\beta s + D_\beta}{A_2 s^4 + B_2 s^3 + C_2 s^2 + D_2 s + E_2} \tag{13}$$

$$\frac{\alpha}{\delta_e}(s) = \frac{A_\alpha s^3 + B_\alpha s^2 + C_\alpha s + D_\alpha}{A_1 s^4 + B_1 s^3 + C_1 s^2 + D_1 s + E_1} \tag{14}$$

Equivalent Time Delay

Time delay in transfer function modeling is used for representing the unmodeled dynamics at higher frequencies then the frequency range of interest and the transportation (for example, measurement) delay in the system. The equivalent term is used for time delay since the high dynamics can be composed of more than one pole and/or zero. Therefore, the total (equivalent) time delay is found by the summation of pole terms and extraction of zero terms. The equation to express equivalent time delay is given as [Tischler, Remple, 2006]:

$$\tau_{eq} \approx \sum_{i=1}^{n} 1/p_i - \sum_{i=1}^{m} 1/z_i \tag{15}$$

Where, τ_{eq}, is the equivalent time delay, $n, m,$ are the order of numerator and denominator, p_i and z_i are the related poles and zeros. Then, the equivalent time delay appears as a frequency-response phase lag:

$$\varphi = -\tau_{eq}\omega \tag{16}$$

Parameter Estimation

After the model structure is built up, the coefficients of transfer function are estimated by using frequency domain system identification tool: CIFER® (Comprehensive Identification from Frequency Responses). CIFER® has a tool named as NAVFIT for transfer function modeling. Another program, Simulink® Parameter Estimation (SimPE), is also used to check and tune the parameters, obtained from CIFER®. Unlike CIFER, SimPE estimates the parameters in time-domain. In both program, same flight data are used. To check the parameters identified by CIFER®, the model structure and the initial conditions for SimPE are taken from CIFER® results. Therefore, the identified transfer function by CIFER is checked by using a different program in a different domain.

Transfer function approach is best suited to SISO (Single-Input-Single-Output) system modeling [Tischler, Remple, 2006]. Therefore, the identification procedure is applied to SISO system in this study.

Longitudinal Transfer Function Modeling

For three DoF longitudinal modeling, two modes dominate the longitudinal dynamics, which are short period and phugoid.

The phugoid mode is a longer period mode where kinetic energy and potential energy are interchanged. Therefore, the oscillation occurs at changing speed, pitch and altitude while angle of attack remains constant. Hodgkinson (1998), approximates the phugoid frequency for subsonic flight as a function of horizontal component of airspeed and the gravitational acceleration. He also approximates the damping of phugoid mode as the drag of the aircraft, which is normally very low. Short-period mode is an underdamped mode where the oscillation lasts only a few seconds. The transient changes and oscillations are seen in pitch, normal load factor and especially in angle of attack. Since short period mode lasts few seconds, it is assumed that the speed does not change during short period mode. The transfer function is modeled as [Hodgkinson, 1998]:

$$\frac{\alpha}{\delta_e}(s) = \frac{M_{\delta_e}}{(s^2 + \zeta_{sp}\omega_{sp}s + \omega_{sp}^2)} \tag{17}$$

Then the model structure for $\alpha/\delta e$ is chosen as given in (17) and for this structure, CIFER estimates the transfer function as given in (18) with cost value obtained using (3):

$$\frac{\alpha}{\delta_e}(s) = \frac{-8.50}{s^2 + 4.05s + 8.96} \tag{18}$$

CIFER cost: *15*

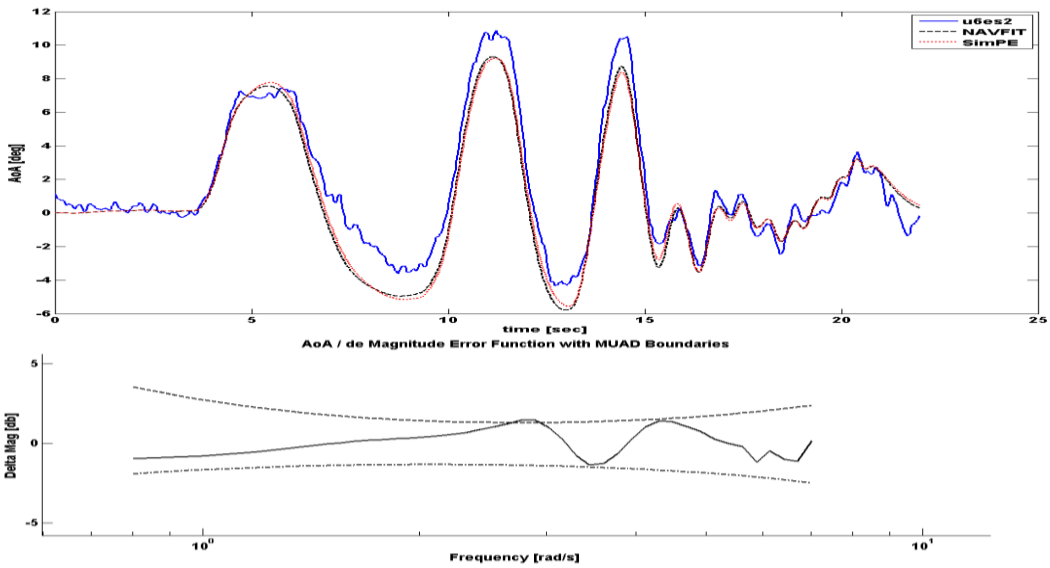

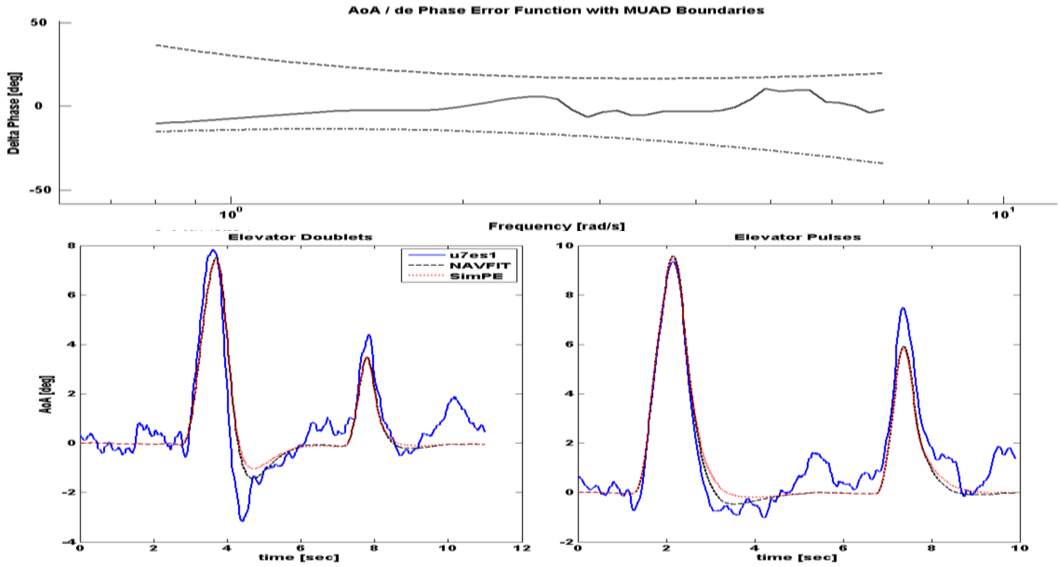

Figure 9: *Angle of Attack Response to Elevator Input (AoA/δe)*

The top graph in Figure 9 shows the flight test data, which are an AoA response to elevator sweep, and responses obtained using estimated transfer functions of NAVFIT and SimPE. The aim of this graph is to show the time domain verification of the identified model with the input used in the identification.

The second and third graphs show the magnitude and phase error between the identified model and flight test data, with MUAD boundaries. In MUAD boundaries, the error between the real A/C dynamic and identified dynamic in the specified frequency range is not detectable to pilots. That means a model within MUAD boundaries is a proper model to use in pilot training and handling quality analysis. The graphs also show that at which frequencies, the identified model matches the real A/C dynamics well.

The two bottom graphs in Figure 9 are time domain verification of identified model with flight test data. The difference with first graph is that, in these graphs doublets and pulses are used as inputs. It may be observed from these graphs that the identified transfer function for AoA response to elevator input matches fairly well with real A/C responses. Moreover, the identified responses are within the MUAD boundaries in the frequency range of interest.

Lateral-Directional Transfer Function Modeling

If the transfer function model structure decided is applied to NAVFIT®, the following result for p/δ_a is obtained:

$$\frac{p}{\delta_a}(s) = \frac{-27.6s^3 - 133.9s^2 + 22.7s + 551.4}{s^4 + 8.4s^3 + 36.7s^2 - 62.8s - 192.5} \tag{19}$$

The resulting cost, using Eqn. (3) as calculated by CIFER program is 6. The equation written as pole zero representation show that the system has an unstable root, which is not realistic:

$$\frac{p}{\delta_a}(s) = \frac{-27.6(s - 1.79)(s^2 - 6.65s^2 + 11.12)}{(s + 2.34)(s - 1.79)(s^2 - 8.95s^2 + 45.82)} \tag{20}$$

Although the classical flight mechanics approach defines roll rate response with the model structure given in Eqn. (12), Figure 10 shows that the identification result based on this structure does not match with the flight data. Therefore, the model structure is reconsidered. The new model is formed according to dominant dynamic modes. For lateral motion, the relation between input and output is defined by roll mode, dutch-roll mode, and spiral mode. The representations of the transfer functions in terms of modes are given as:

$$\frac{p}{\delta_a}(s) = \frac{K_\emptyset s(s^2 + \zeta_\emptyset \omega_\emptyset s + \omega_\emptyset^2)}{(T_R s + 1)(T_s s + 1)(s^2 + \zeta_d \omega_{n_d} s + \omega_{nd}^2)} \tag{21}$$

$$\frac{\beta}{\delta_r}(s) = \frac{K_{\beta_r}(T_{\beta_{r1}}s+1)(T_{\beta_{r2}}s+1)(T_{\beta_{r3}}s+1)}{(T_R s+1)(T_s s+1)(s^2+\zeta_d\omega_{n_d}s+\omega_{n_d}^2)} \tag{22}$$

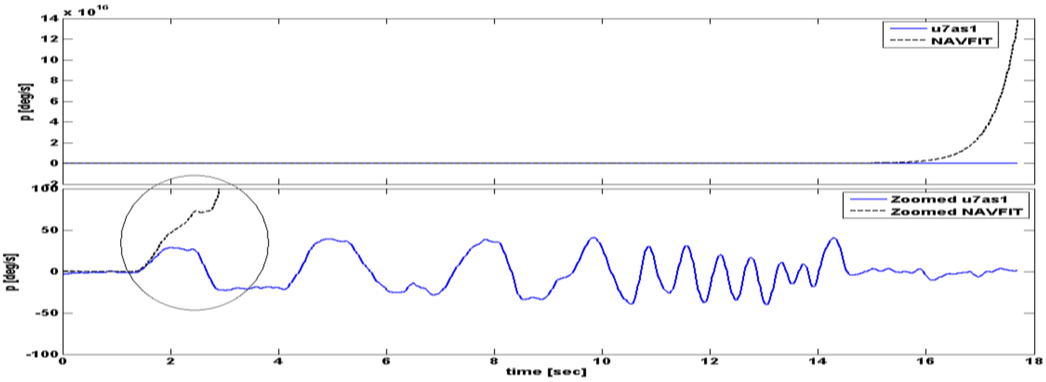

Figure 10: *Roll Rate Response to Aileron Input (p/δa) CIFER Result*

If the roll and sideslip dynamics are assumed to be completely decoupled [Hodgkinson, 1998], then it is assumed that rolling motion is created by only aileron input and dutch-roll motion (with no roll rate) is created by rudder input. Therefore, the relation between roll rate and aileron deflection, and the relation between sideslip and rudder deflection may be written as [Bischoff, Palmer, 1982]

$$\frac{p}{\delta_a}(s) = \frac{L_{\delta_a}}{s-L_p} \tag{23}$$

$$\frac{\beta}{\delta_r}(s) = \frac{Y_{\delta_r}}{s^2+(-Y_v-N_r)s+N_\beta} \tag{24}$$

Then the estimated transfer functions by CIFER and SimPE software are given in Eqn. (25) with the associated cost function below:

$$\frac{p}{\delta_a}(s) = \frac{-33.1996}{s+9.5967} \qquad \frac{p}{\delta_a}(s) = \frac{-29.418}{s+8.7068} \tag{25}$$

CIFER cost: *61* SimPE cost: *65*

SimPE results are very close to results of CIFER, because CIFER results are used as initial conditions of SimPE. Since SimPE use different domain and identification method, the results obtained SimPE can slightly differ from CIFER results, although transfer function estimated by CIFER is true. When the model structure for β/δ_r is chosen as in Eqn. (24) then the estimated transfer functions for this structure are given in Eqn. (26) with associated cost values.

$$\frac{\beta}{\delta_r}(s) = \frac{-9.16}{s^2+1.68s+13.32} \qquad \frac{\beta}{\delta_r}(s) = \frac{-8.48}{s^2+1.38s+12.89} \tag{26}$$

CIFER cost: *38* SimPE cost: *46*

So far, the roll mode and dutch-roll mode are identified separately by using a suitable transfer function models with low cost values. In this part, spiral mode identification presented. If the poles of the identified roll mode and Dutch roll mode are written in Eqn. (22), the Eqn. (27) is obtained:

$$\frac{p}{\delta_a}(s) = \frac{K_\emptyset s(s^2+\zeta_\emptyset\omega_\emptyset s+\omega_\emptyset^2)}{(s+9.5967)(s+{}^1/_{T_s})(s^2+1.38s+12.89)} \tag{27}$$

When the numerator and denominator expanded, the expression in (28) is obtained:

$$\frac{p}{\delta_a}(s) = \frac{A_1s^3+B_1s^2+C_1s+D_1}{s^4+(10.1+C_s)s^3+(24.9+10.1C_s)s^2+(112.3+24.9C_s)s+112.3C_s} \tag{28}$$

NAVFIT is not capable to identify a parameter in simplified expression of a polynomial (i.e., T_s term in Eqn. (27)). To overcome this, Tischler suggests using arithmetic manipulation of the frequency-response functions at each identification frequency ω [Tischler, Remple, 2006]. The example of this is given as:

$$(s^2 + \zeta_d \omega_{n_d} s + \omega_{n_d}^2)\frac{p}{\delta_a}(s) = \frac{L_\emptyset s(s^2 + \zeta_\emptyset \omega_\emptyset s + \omega_\emptyset^2)}{(s + {}^1/_{T_r})(s + {}^1/_{T_s})} \quad (29)$$

To estimate a mode using (29), obtaining of the proper frequency response function is required. It is also required that to obtain a proper frequency response, one applies the windowing and chirp z transformation, which means that all the calculations carried out by FRESPID tool of CIFER must be done by the user. Moreover, COMPOSITE toll, one of the advantages of CIFER, cannot be used. Therefore, applying this procedure counteracts the productivity and advantages of the program.

For these reasons, identifying spiral mode using SimPE is more suitable. To estimate that mode, C_s is setting as free parameter for estimation. Moreover, coefficients of the numerator part are setting as free parameter to estimate the numerator of p/δ_a. The estimated transfer function is given in Eqn. (30).

$$C_s = {}^1/_{T_s} = 1.73\, rad/s$$

$$\frac{p}{\delta_a}(s) = \frac{-30.874s^3 - 110.63s^2 - 436.92s - 769.92}{s^4 + 11.82s^3 + 42.42s^2 + 155.47s + 194.40} \quad (30)$$

SimPE cost: *38*

The top graph in Figure 11 shows the flight test data, which is a roll rate response to aileron sweep, and responses obtained using estimated transfer functions of NAVFIT and SimPE. The aim of this graph is to show the time domain verification of the identified model by the input used in the identification. The second and third graphs show the magnitude and phase error between the identified model and flight test data, with MUAD boundaries, as explained previously. The bottom two graphs are the time domain verification of identified model with flight test data. The difference with the top graph is that in these graphs doublet inputs and pulses are employed as inputs. From these two last graphs, it may be concluded that the estimated model performs well with verification inputs as well. The magnitude error and phase error are within the MUAD boundaries.

The denominator in Eqn. (30) is a common denominator of for lateral/directional motion. By taking this denominator constant, numerator of β/δ_r is obtained using CIFER and SimPE. The identified transfer functions are given as:

$$\frac{\beta}{\delta_r}(s) = \frac{10.34s^2 + 85.57s - 145.67}{s^4 + 11.82s^3 + 42.42s^2 + 155.47s + 194.40} \quad (31)$$

CIFER cost: *41*

$$\frac{\beta}{\delta_r}(s) = \frac{7.17s^2 + 87.75s + 127.51}{s^4 + 11.82s^3 + 42.42s^2 + 155.47s + 194.40} \quad (32)$$

SimPE cost: *24*

It may be observed from Figure 12 that, the identification time histories (top graph) match fairly well with the flight test data. However, in the magnitude error graph and phase error graph, some points are beyond the MUAD boundaries (1 dB and 9 degrees maximum). This may be due to the fact that those frequencies have not been excited by the input.

The evaluation of obtained results from transfer function modeling is summarized as the linear model obtained from system identification matches with flight data considerably well. For example, when Figure 9 and Figure 12 are seen, it is noticed that estimations of AoA and AoS match up to high angles like 10°.

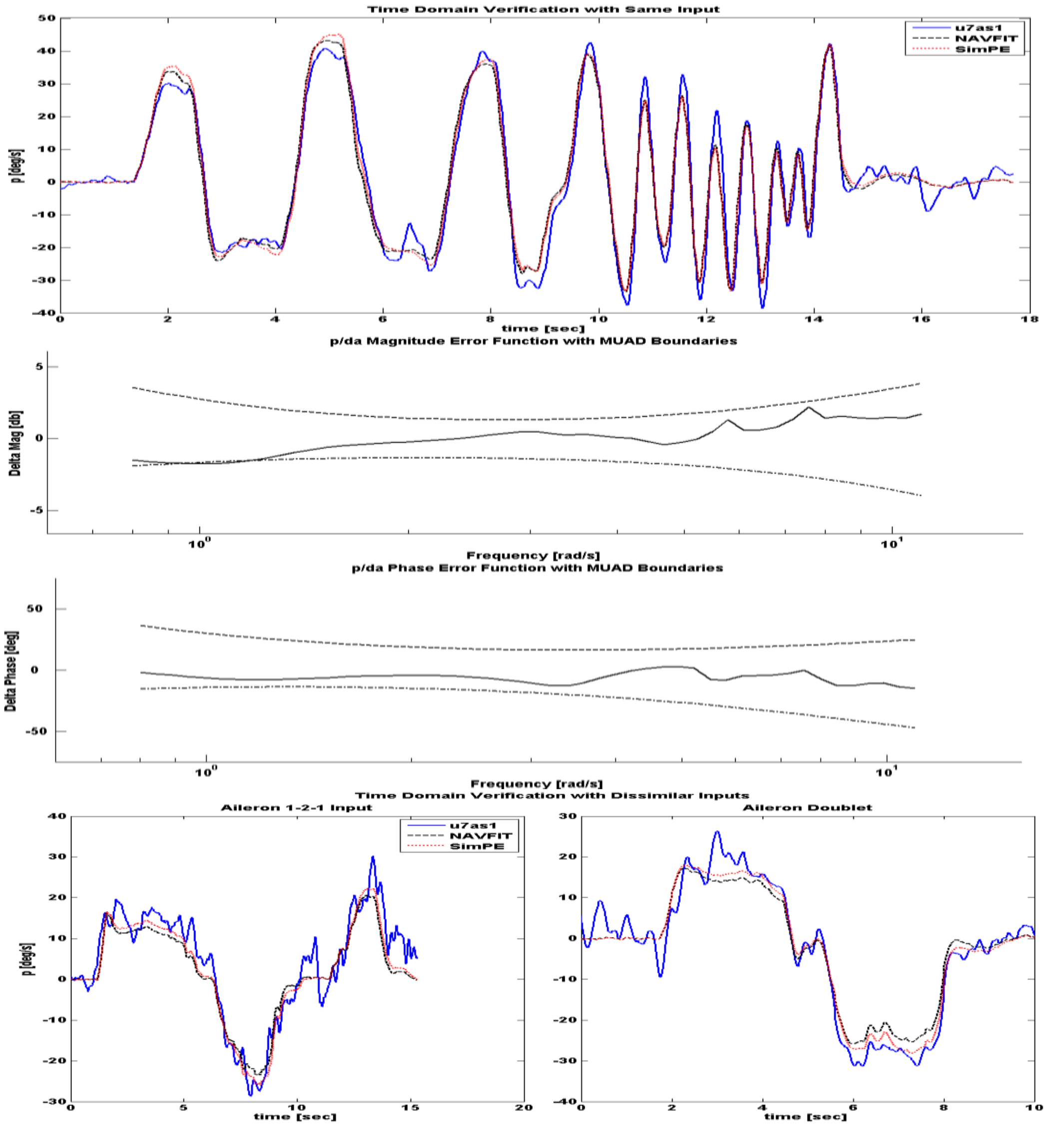

Figure 11: *Roll Rate Response to Aileron Input (p/δa)*

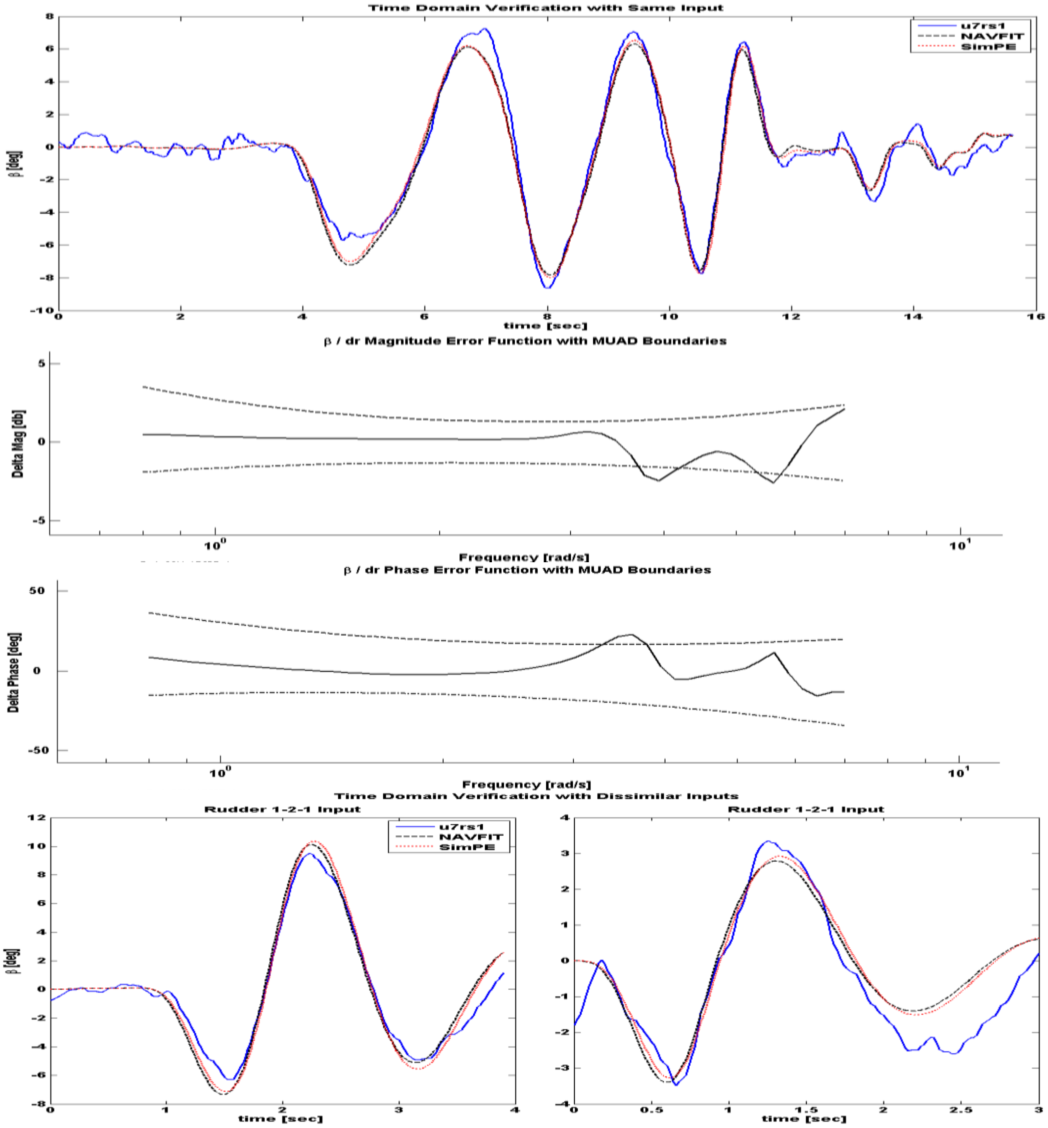

Figure 12: *Sideslip Response to Rudder Input (β/δr)*

Handling Quality Analysis

Handling quality analysis is done by using the identified transfer functions and procedure given in a flying quality document [Prosser, Wiler, 1976]. The handling quality requirements are specified by concerning vehicle class and flight phase category. The vehicle class of Pelikan is Class 1. The flight phase category is Category B.

According to vehicle class and flight phase category of Pelikan, the levels of flying qualities for longitudinal motion given in Table 3, together with the requirements.

Table 3: *Longitudinal Response Characteristics*

	Level	Flight Phase Category	Class	Min ζ_{sp}	Max ζ_{sp}	*Pelikan*
SHORT-PERIOD	1	B	I	0.30	2.00	
	2	B	I	0.20	2.00	*1.35*
	3	B	I	0.15	-	

As seen in Table 3, the level of short period damping is Level 1. From Eqn. (18), the short period frequency is found as 3 rad/s, which makes it Level 1.

Table 4: *Lateral-Directional Response Characteristics*

	Level	Flight Phase Category	Class	Min ζ_d	*Pelikan*	Min $\zeta_d\omega_{nd}$	*Pelikan*	Min ω_{nd}	*Pelikan*
DUTCH-ROLL	1	B	I	0.08		0.15		1.0	
	2	B	I	0.02	*0.193*	0.05	*0.692*	0.4	*3.591*
	3	B	I	0.02		-		0.4	
	Level	Flight Phase Category	Class	Max T_r	*Pelikan*				
ROLL	1	B	I	1.4					
	2	B	I	3	*0.193*				
	3	B	I	10					
	Level	Flight Phase Category	Class	Min t_{double}	*Pelikan*				
SPIRAL	1	B	I	20					
	2	B	I	12	*2.5*				
	3	B	I	4					

Requirements for lateral/directional motion together with Pelikan results are given in Table 4. As seen from the table, the Dutch-roll and roll response characteristics are in Level 1. Spiral mode of Pelikan does not match the acceptable levels of handling qualities.

CONCLUSIONS

In this study, flight mechanics model of a UAV using flight test data is obtained. The process covers performing flight test, collecting and reconstructing the data, spectral analysis of data and frequency domain system identification using transfer function modeling.

The flight tests are performed using specific inputs to excite the longitudinal and lateral/directional modes of the UAV. In the flight tests, piloted frequency sweeps are used as identification inputs and piloted doublets and 1-2-1 inputs are used as verification inputs. Data consistency is checked by applying output error method. This method gives bias and scale factor corrections for especially angle of attack and angle of sideslip in this study. Using CIFER®, which is an effective frequency domain system identification tool, system identification process is applied. SimPE is used to check the obtained results of CIFER and is used in parameter estimation.

The estimated transfer functions are used to evaluate the handling qualities of the aircraft. The studies show that flight testing and system identification is an effective way to obtain the models of UAV.

References

Bischoff, D. E., and Palmer, R. E*., Investigation of Low Order Lateral Directional, Transfer Function Models for Augmented Aircraft*, AIAA Guidance and Control Conference, Paper 82-1610, Aug. 1982, pp. 579-586.

Graham, D., and McRuer, D.T. (1971), *Analysis of Nonlinear Control Systems*, Dover, NY.

Jategaonkar, R.V. (2006), *Flight Vehicle System Identification: A Time Domain Methodology*, AIAA Inc., Reston, VA.

Hodgkinson, J. (1998), *Aircraft Handling Qualities*, AIAA Inc., Reston, VA.

Klein, V., and Morelli, E. A. (2006), *Aircraft System Identification: Theory and Practice*, AIAA Inc., Reston, VA.

Klein, V (1977), *Compatibility Check of Measured Aircraft Responses Using Kinematic Equations and Extended Kalman Filter*, NASA TN D-8514, Washington D.C.

Morelli, E.A. (2000), *Identification of Low Order Equivalent System Models from Flight Test Data,* NASA/TM-2000-210117, NASA, VA.

Morelli, E. A. (2003), *Low Order Equivalent System Identification for the Tu-144LL Supersonic Transport Aircraft*, Journal of Guidance, Control, and Dynamics, Vol. 26, No. 2, pp. 354-362.

Prosser, C. F., and Wiler, C.D, *RPV Flying Qualities Design Criteria*, AFFDL-TR-76-125., WPAFB, OH, 1976.

Roskam, J., *Airplane Flight Dynamics and Automatic Flight Controls,* DARcorporation, Lawrence, KS. Prentice Hall Inc., Upper Saddle River, NJ, 2001

Schoukens, J., Pintelon R., and Van Hamme (1994), H., *Identification of linear dynamic systems using piecewise constant excitations: Use, misuse and alternatives,* Automatica, Vol. 30, NO. 7, pp 1153-1169.

Schoukens, J., Rolain Y., Pintelon, R. (2006), *Leakage Reduction in Frequency-Response Function Measurement*, IEEE Transactions on Instrumentation and Measurement, Vol. 55, NO. 6, pp.2286-2291

Tischler, M. B., and Remple, R.K. (2006) *Aircraft and Rotorcraft System Identification: Engineering Methods with Flight-Test Examples*, AIAA Inc., Reston, VA.

U. S. Department of Defense, *Dictionary of Military and Associated Terms*, Joint Publication 1-02, 2001, p. 557.

Williams, J.N., Ham J.A., and Tischler M.B., *Flight Test Manual: Rotorcraft Frequency Domain Flight Testing*, Airworthiness Qualification Test Directorate, California, CA, 1995